

# Stationary Premixed Flames in Spherical and Cylindrical Geometries

P. D. Ronney\*

University of Southern California, Los Angeles, California 90089  
and

K. N. Whaling,† A. Abbud-Madrid,‡ J. L. Gatto,§ and V. L. Pisowicz¶  
Princeton University, Princeton, New Jersey 08544

Stationary source-free spherical flames ("flame balls") in premixed combustible gases were studied by employing low-gravity ( $\mu g$ ) environments in a drop tower and an aircraft flying parabolic trajectories to diminish the impact of buoyancy-induced convective flow. Flame balls were found in all mixture families tested when 1) the Lewis number  $Le$  of the deficient reactant was sufficiently low and 2) the compositions were sufficiently close to the flammability limits. Probably as a consequence of the reduction in buoyant convection, the flammability limits at  $\mu g$  were significantly more dilute than those at Earth gravity; for example, 3.35%  $H_2$  vs 4.0%  $H_2$  in lean  $H_2$ -air mixtures. By comparison with analytical and computational models, it is inferred that the phenomenon is probably related to diffusive-thermal effects in low- $Le$  mixtures in conjunction with flame-front curvature and radiative heat losses from the combustion products. The chemical reaction mechanism appears to play no *qualitative* role. In the aircraft experiments, the gravity levels ( $\approx 10^{-2}g_0$ ) were found to cause noticeable motion of flame balls due to buoyancy, which in turn influenced the behavior of flame balls. At these  $g$  levels, a new type of transient, nearly cylindrical flame structure, termed "flame strings," was observed.

## Nomenclature

$D$  = mass diffusivity  
 $E$  = overall activation energy of chemical reaction  
 $Fr$  = Froude number  
 $g$  = acceleration of gravity  
 $g_0$  = Earth gravity  
 $Le$  = Lewis number  
 $P$  = pressure  
 $R$  = radius of flame ball  
 $\mathcal{R}$  = gas constant  
 $r$  = radial coordinate  
 $T$  = temperature  
 $T_{ad}$  = adiabatic combustion temperature of homogeneous mixture  
 $T_b$  = adiabatic temperature of flame ball  
 $T_*$  = temperature at flame ball surface  
 $V$  = drift velocity of flame ball  
 $\alpha$  = thermal diffusivity  
 $\beta$  = nondimensional activation energy,  $\equiv E/\mathcal{R}T$   
 $\mu g$  = microgravity  
 $\rho$  = gas density  
 $\phi$  = equivalence ratio  
 $\phi_c$  = critical equivalence ratio,  $\equiv Le_{fu}/Le_{ox}$

## Subscripts

$fu$  = fuel  
 $ox$  = oxidizer  
 $0$  = ambient conditions

## I. Introduction

### A. Prior Work

NEARLY 50 years ago, Zeldovich<sup>1</sup> showed the possibility of stationary spherical flames existing in premixed gases. These structures, which we term "flame balls," were predicted to exist for every combustible mixture, just as the same governing equations in planar geometry admit a steadily propagating flame as a solution for every mixture. In the former case the solutions are characterized by a radius and in the latter case by the burning velocity. Subsequent analyses<sup>2,3</sup> showed that flame balls are probably unstable and thus are not physically observable, just as planar flames are frequently subject to instabilities that prevent them from remaining planar.

Until recently, the only experimentally observed flame structures that resembled flame balls were rising cap-shaped flames, having a typical diameter of 0.4 cm, found in lean hydrogen-oxygen-diluent mixtures near flammability limits.<sup>4,5</sup> These "flame caps" rise due to buoyancy, and thus buoyant convection has been suggested as a stabilizing mechanism.<sup>6,7</sup> Moreover, flame caps have only been observed in lean hydrogen-oxygen-diluent mixtures, suggesting that a low Lewis number of the stoichiometrically deficient reactant, defined as

$$Le_i \equiv \frac{\text{thermal diffusivity of the bulk mixture}}{\text{mass diffusivity of reactant } i \text{ into the bulk mixture}} = \frac{\alpha}{D_i} \quad (1)$$

is necessary for their existence.

To search for potential stabilizing mechanisms other than buoyancy for flame balls in low- $Le$  mixtures, we have studied<sup>8</sup> freely propagating flames in lean  $H_2$ -air mixtures in a reduced-gravity or "microgravity" ( $\mu g$ ) environment obtained in a drop tower. The following sequence of phenomena was ob-

Received Dec. 15, 1992; revision received July 23, 1993; accepted for publication July 26, 1993. Copyright © 1993 by P. D. Ronney, K. N. Whaling, A. Abbud-Madrid, J. L. Gatto, V. L. Pisowicz. Published by the American Institute of Aeronautics and Astronautics, Inc., with permission.

\*Research Associate Professor, Department of Mechanical Engineering. Member AIAA.

†Graduate Student, Department of Mechanical and Aerospace Engineering; currently at GE Aircraft Engines, Cincinnati, OH 44215.

‡Graduate Student, Department of Mechanical and Aerospace Engineering; currently at Department of Mechanical Engineering, University of Colorado, Boulder, CO 80309.

§Graduate Student, Department of Mechanical and Aerospace Engineering.

¶Undergraduate Student, Department of Mechanical and Aerospace Engineering.

served as the mixtures were progressively diluted with small amounts of a chemical inhibitor and "coloring agent" ( $\text{CF}_3\text{Br}$ ) or larger amounts of excess air. For mixtures not too close to the flammability limits, expanding cellular flame fronts, qualitatively similar to those observed<sup>9</sup> at Earth gravity (1 g), were found. For more dilute mixtures, i.e., closer to the limits, the cell division occurred only at early times in the flame development, and subsequently the nondividing cells drifted apart from each other without apparent interaction. For still more dilute mixtures, these cells formed seemingly stable flame balls with typical radii of 0.5 cm. The drift velocity of the flame balls decreased to less than 0.1 cm/s by the end of the drop test, but the limited duration of available  $\mu\text{g}$  (2.2 s) precluded definite conclusions concerning their stability and mobility. For each mixture, the flame balls exhibited a bimodal size distribution. The difference between the radii of the large and small flame balls decreased with increasing dilution until a nearly unimodal distribution was observed at the flammability limit.

These phenomena have not been observed in mixtures with  $Le$  close to or greater than unity. Instead, conventional propagating flames and self-extinguishing flames<sup>10,11</sup> are observed at  $\mu\text{g}$  under these conditions.

## B. Comparison of Models with Experiments

The experiments indicate the probable existence of flame balls but do not conclusively identify a stabilizing mechanism or explain why they seem to exist only for a narrow range of compositions. The central role of dilution in these phenomena suggests that radiant heat losses may exert a controlling influence. The impact of heat loss depends on the ratio of a characteristic heat production rate to a characteristic loss rate.<sup>12</sup> Increasing dilution decreases the flame temperature, which in turn decreases the characteristic chemical reaction rate more than the characteristic radiative loss rate since the former is generally a stronger function of temperature than the latter, i.e., exponential vs algebraic. Consequently, increasing dilution increases the impact of heat losses, which eventually leads to a flammability limit. In the aforementioned  $\mu\text{g}$  experiments, radiant heat loss could occur via blackbody radiation from soot in the  $\text{CF}_3\text{Br}$ -doped mixtures or via spectral radiation from nonluminous product gases such as  $\text{H}_2\text{O}$ .

Recent analyses<sup>13,14</sup> support this hypothesis. It is predicted that when heat losses are not too strong, two stationary flame ball radii are possible, and when the losses are sufficiently strong, no solutions exist, indicating a flammability limit. As the limit is approached, the difference between the radii of the "large" and "small" balls decreases to zero, which is consistent with the experimental observations.<sup>8</sup> For  $Le$  less than and bounded away from unity, all small flame balls are predicted to be unstable to radial disturbances, and when the heat losses are sufficiently low, the large balls are predicted to be unstable to three-dimensional disturbances. This is consistent with the observation that mixtures far from the limits exhibit continuously splitting cellular flames rather than nonsplitting flame

balls but contradicts the observation that both small and large flame balls appear to be stable near the limits. When  $Le$  is close to unity, all flame balls are predicted<sup>15</sup> to be unstable to radial disturbances, regardless of the level of heat loss. This is consistent with the aforementioned observation that flame balls are not seen in mixtures with  $Le$  close to or larger than unity.

All of the aforementioned theories assumed single-step Arrhenius kinetics with large activation energy, constant thermodynamic and transport properties, and simple radiation properties. Only one numerical simulation of flame balls employing detailed kinetic and transport models has been reported.<sup>16</sup> The computed steady properties of nonadiabatic flame balls in  $\text{H}_2$ -air mixtures were qualitatively consistent with theories in that two solutions were predicted for mixtures having fuel concentrations higher than the limiting value. No transient properties were studied, and hence stability could not be compared to theoretical predictions or experiments.

## II. Objectives and Approach

Although the comparisons between experimental observations and theory are encouraging, there are still several significant unresolved issues concerning the existence and stabilization mechanisms of stationary spherical flames. The goal of the current investigation is to provide experimental observations that enable more complete comparisons with analytical and numerical models.

### A. Increased $\mu\text{g}$ Duration

Probably the most significant limitation of the prior work<sup>8</sup> is the short duration of  $\mu\text{g}$  (2.2 s). This causes uncertainty as to whether any flame balls are actually stable or would eventually extinguish, expand, or split given sufficient  $\mu\text{g}$  duration. Also, small flame balls seemed stable in these short-duration experiments, whereas theory predicts instability. Consequently, a primary objective of the current work was to observe the stability and evolution of flame balls for a longer duration of  $\mu\text{g}$ .

To satisfy this objective, an aircraft flying parabolic trajectories was employed. This provided a low-gravity duration about 10 times greater than that provided by the drop tower. The use of the aircraft also enabled the use of a video imaging system that allowed visualization of flames in  $\text{H}_2$ - $\text{O}_2$ -diluent mixtures without  $\text{CF}_3\text{Br}$ . This facilitates comparison with numerical models of flame balls,<sup>16</sup> since the chemical, transport, and radiative properties of  $\text{CF}_3\text{Br}$ -free  $\text{H}_2$ - $\text{O}_2$ -diluent mixtures are much better known than those properties in mixtures seeded with  $\text{CF}_3\text{Br}$ . This imaging system could not be employed in drop-tower tests because of the high impact loads that terminate these tests.

### B. Effects of Chemical and Transport Properties

Before this work, only one family of mixtures probably exhibiting flame balls had been found (lean  $\text{H}_2$ -air). The influ-

Table 1 Computed properties of the mixture families investigated<sup>a</sup>

Fuel	Diluent	$\phi$	$\phi_c$	$Le_{fu}$	$Le_{ox}$	Mole % fuel at flammability limit	$T_{ad}$ at flammability limit, K	Mole % fuel at stability limit
$\text{H}_2$	Air	Varies	0.32	0.29	0.91	$3.35 \pm 0.05$	577	$3.6 \pm 0.1$
$\text{H}_2$	Ar	0.25	0.27	0.29	1.07	$2.40 \pm 0.05$	571	$2.6 \pm 0.2$
$\text{H}_2$	$\text{CO}_2$	0.25	0.30	0.19	0.63	$4.6 \pm 0.1$	575	$5.2 \pm 0.1$
$\text{H}_2$	$\text{SF}_6$	0.25	0.31	0.06	0.19	$6.5 \pm 0.1$	464	$8.7 \pm 0.5$
$\text{CH}_4$	$\text{SF}_6$	1.00	1.13	0.27	0.24	$10.2 \pm 0.2$	1050	$10.9 \pm 0.2$

<sup>a</sup>For the lean  $\text{H}_2$ -air mixtures,  $\phi$  varies but is much less than  $\phi_c$  for all mixtures tested. The values of  $Le_{fu}$  and  $Le_{ox}$  are computed using standard techniques.<sup>33</sup> Though  $Le$  is only slightly dependent on temperature, the reported values are temperature averaged between 300 K and the measured near-limit flame front temperatures of  $\approx 1000$  K for  $\text{H}_2$  flames and  $\approx 1500$  K for  $\text{CH}_4$  flames. Also shown are measured flammability limits at 1-atm initial pressure with no added  $\text{CF}_3\text{Br}$ , the corresponding calculated adiabatic flame temperatures, and the flame ball stability limits.

ence of variations in  $Le$ , chemical properties, and radiative properties on flame balls had not been assessed. This is potentially significant because, for example, it might be argued that flame balls are a unique feature of the chemistry or radiative spectra of  $H_2$ -air flames. Also, in the mixtures tested, a small amount of  $CF_3Br$  was added to render the  $H_2$ -air flames luminous, thereby enabling direct photography. The qualitative effect of  $CF_3Br$  on flame ball behavior was argued to be minor,<sup>8</sup> but testing this assertion is desirable. Hence, there is a need to study mixtures having a wider range of chemical and transport properties.

A summary of the characteristics of the mixture families employed to fulfill this need is given in Table 1. For comparison with previous results,<sup>8</sup> lean  $H_2$ -air mixtures were studied. Lean ( $\phi = 0.25$ )  $H_2$ - $O_2$ -Ar mixtures were studied because their chemical properties and Lewis numbers are similar to  $H_2$ -air mixtures. Mixtures of lean ( $\phi = 0.25$ )  $H_2$ - $O_2$ - $CO_2$  and lean ( $\phi = 0.25$ )  $H_2$ - $O_2$ - $SF_6$  were studied to obtain very low  $Le_{fu}$ . In these cases  $\phi = 0.25$  was chosen because it was less than the critical value described in the following section but was not so low that much excess  $O_2$  was present; this would raise  $\alpha$  and thus  $Le_{fu}$ . Additionally, these families of mixtures provided a range of radiation intensities and spectra. Flame chemistry effects were tested by employing stoichiometric ( $\phi = 1.00$ )  $CH_4$ - $O_2$ - $SF_6$  mixtures. These mixtures were chosen because  $CH_4$  has the lowest molecular weight and thus highest  $D$  of any fuel with chemical properties different from  $H_2$  and because  $SF_6$  is probably the only diluent gas that has sufficiently low  $\alpha$  to provide low  $Le_{fu}$  while being fairly inert at near-limit combustion temperatures (i.e., the rate of radical attack on  $SF_6$  at combustion temperatures is much lower than the rate of radical attack on  $CH_4$  or  $O_2$ <sup>17,18</sup>). Stoichiometric  $CH_4$ - $O_2$ - $SF_6$  mixtures were chosen because  $Le_{fu} \approx Le_{ox}$ , and hence the distinction between "deficient" and "abundant" reactants is unimportant, and because stoichiometric mixtures minimize the quantity of "light" fuel or oxidant, thus minimizing  $\alpha$  and therefore  $Le_{fu}$  and  $Le_{ox}$ .

### C. Effects of Equivalence Ratio

Another theoretical prediction that had not been tested experimentally before this work is the effect of  $\phi$ . Transition from fuel-lean burning to fuel-rich burning at the flame ball surface is predicted<sup>19</sup> to occur not at  $\phi = 1$  as in planar flames<sup>12</sup> but rather at  $\phi = \phi_c \equiv Le_{fu}/Le_{ox}$ . Hence, when  $\phi$  is significantly less than (greater than)  $\phi_c$ , the fuel (oxidant) is

the "deficient reactant" for the purposes of estimating the effective  $Le$ . As a consequence, significant changes in flame ball behavior are predicted near  $\phi = \phi_c$ , with no significant change near  $\phi = 1$ . An experimental test of this interesting prediction is desirable.

Consequently, a set of near-limit  $H_2$ - $O_2$ - $N_2$  mixtures with a fixed mole fraction of  $H_2$  was tested for a range of  $\phi$  spanning  $\phi_c$ . Since  $O_2$  and  $N_2$  have virtually identical thermodynamic and diffusive properties,  $T_{ad}$  and the Lewis numbers are essentially independent of  $\phi$ . Also, neither  $O_2$  nor  $N_2$  radiate significantly at the temperatures of interest. Thus, in  $H_2$ - $O_2$ - $N_2$  mixtures with a fixed mole fraction of  $H_2$ ,  $\phi$  can be adjusted without influencing other chemical or transport properties significantly.

### D. Test of Models of Cellular Flame Formation

There are two conflicting models of the instability that lead to the cellular structures observed in mixtures not too close to the flammability limit. A test of these models is relevant to the current study because the cellular instability seems to affect the formation of flame balls. One model is the "diffusive-thermal" model, which predicts that cellular flames occur when  $Le$  of the stoichiometrically deficient reactant is sufficiently low.<sup>12,20</sup> The other model is the "preferential diffusion" model,<sup>5,21</sup> which predicts that cellular flames occur when the more rapidly diffusing reactant is the deficient one, regardless of  $Le$ . Although a computational study<sup>22</sup> of flames in  $H_2$ - $O_2$ - $N_2$  mixtures, in which the mass diffusivities of  $H_2$  and  $O_2$  were artificially manipulated, supported the diffusive-thermal hypothesis, no experimental test of these two competing models had been reported before this work. In this context it should be noted that most experiments on cellular flames have employed fuel- $O_2$  mixtures diluted with  $N_2$ . In this case it is difficult to separate diffusive-thermal from preferential diffusion effects because the mass diffusivity of  $O_2$  in  $N_2$  is comparable to the thermal diffusivity of  $N_2$ .

To compare these conflicting models,  $H_2$ - $O_2$ - $SF_6$  mixtures were tested at  $\phi = 2$  in addition to the  $\phi = 0.25$  mixtures discussed earlier. According to diffusive-thermal theories, cellular flames should be observed in these mixtures for all values of  $\phi$  because both  $Le_{fu}$  and  $Le_{ox}$  are significantly less than unity (cf. Table 1), whereas preferential diffusion models would predict cellular flames only at low  $\phi$  since  $H_2$  is the more diffusive reactant.

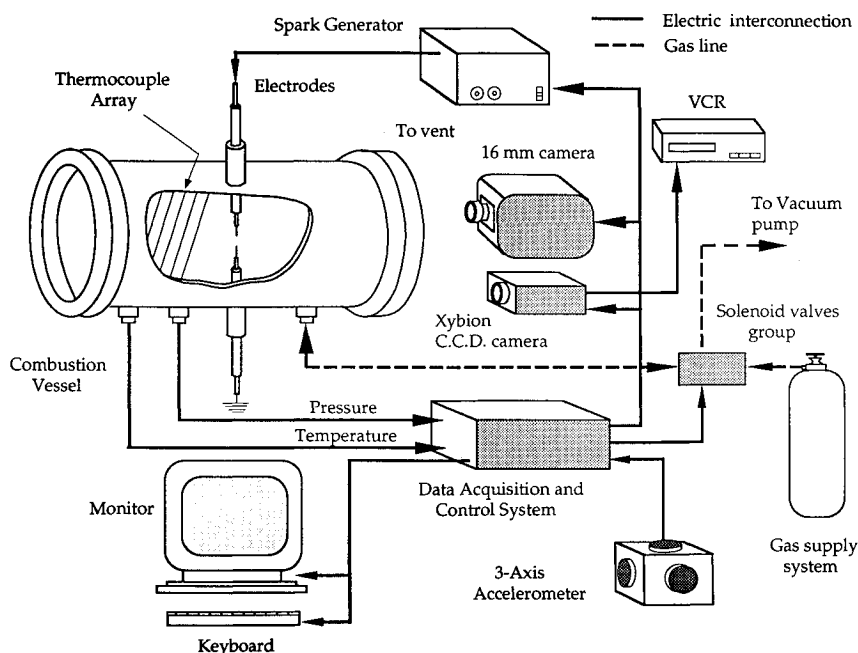


Fig. 1 Experimental apparatus block diagram.

### III. Experimental Apparatus and Procedures

The experimental apparatus (Fig. 1) consisted of a cylindrical combustion vessel of 25-cm diameter and 25-cm length having transparent end windows, a spark generator, a 16-mm motion picture camera, an intensified charge-coupled device (CCD) array video imaging system (aircraft tests only), an array of thermocouples having 50- $\mu\text{m}$  wire diameter and 100- $\mu\text{m}$  bead diameter, a 3-axis accelerometer (aircraft tests only), and a data acquisition and control system (DACS). Chromel-alumel thermocouples were chosen because they exhibited no apparent catalytic effect in  $\text{H}_2\text{-O}_2$ -diluent mixtures. The DACS controlled the spark generator and cameras and collected data from the thermocouples and accelerometers. The spark generator provided at least 2 J of ignition energy in less than 25 ms. Ignition was commanded only after low-gravity conditions were attained. Gas compositions were determined by partial pressures. The estimated uncertainty of the composition was  $\pm 1.5\%$  of each component, e.g.,  $4.00 \pm 0.06\%$   $\text{H}_2$  in air. All results were obtained at an initial temperature of  $300 \pm 5$  K and, except where noted, an initial pressure of 1 atm.

For initial tests, the NASA Lewis Research Center drop tower<sup>23</sup> was employed, which provided 2.2 s of reduced gravity ( $\approx 10^{-5}g_0$ ). In the drop tower tests employing  $\text{H}_2\text{-O}_2$ -diluent mixtures, typically 1% by volume of  $\text{CF}_3\text{Br}$  was added to enable direct photography. NASA's KC-135A low-gravity research aircraft<sup>23</sup> was used for further tests, providing up to 25 s of lower quality reduced gravity, typically  $\pm 0.02g_0$ . The component of acceleration aligned with the spark electrodes was found to exhibit much higher  $g$  levels than the other two components. Experiments were conducted during 16 test flights averaging 40 low-gravity parabolic trajectories per flight. During the course of these flights, most test conditions were repeated several times. It was found that the measured flammability limits, stability properties, and flame ball radii were quite consistent between experiments.

The imaging system, which is similar to that described in Ref. 24, was an intensified CCD array video camera (Xybion Systems ISG-240) having a sensitivity of  $< 10^{-7}$  ft-c faceplate illumination and significant response at wavelengths from 400 to 900 nm. This camera proved capable of imaging flames in all mixture families tested, including the  $\text{CF}_3\text{Br}$ -free  $\text{H}_2\text{-O}_2$ -diluent mixtures that are not visible to the naked eye or conventional photography. Although no detailed spectroscopic measurements were attempted in this work, the strongest detectable band in the  $\text{H}_2\text{-O}_2$ -diluent mixtures was probably the near-IR band of hot  $\text{H}_2\text{O}$  centered at 823 nm.<sup>25</sup> Consistent with this hypothesis is the fact that images of flames in these mixtures taken with and without a 700-nm long-pass filter were nearly identical.

To determine flame ball or cell radii, video records were analyzed on a digital image processing system. Where available, film records were converted to video images and analyzed in the same way. Figure 2 shows an example of the emission intensity profile of a flame ball in a  $\text{CF}_3\text{Br}$ -free  $\text{H}_2$ -air mixture. The flame ball or cell radius was arbitrarily defined as half the width of the intensity profile at one-third of the peak intensity, which generally corresponded closely to the radius inferred by visual inspection of the video images.

With only one axial camera view, distances from the object analyzed to the imaging system cannot be discerned; geometrical considerations dictate that an uncertainty of  $\pm 15\%$  in feature size results. An orthogonal view would have been useful, but space and cost constraints precluded this option in the current work.

## IV. Results and Discussion

### A. Qualitative Observations

#### 1. Drop-Tower Tests

In the drop-tower tests, all low  $Le$  mixtures followed the same sequence of behavior as dilution was increased as was

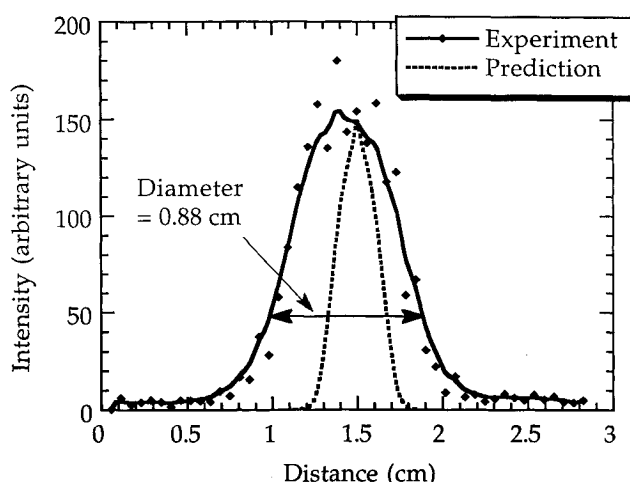


Fig. 2 Example of the emission intensity profile of an isolated flame ball in a  $\text{CF}_3\text{Br}$ -free 3.5%  $\text{H}_2$ -air mixture (solid curve) and comparison with estimate based on numerical simulations<sup>16</sup> (dotted curve).

found for lean  $\text{H}_2$ -air mixtures described in Sec. I.A. As in the previous study,<sup>8</sup> the size distribution of flame balls was somewhat bimodal, and both large and small balls seemed stable. However, examination of the film records again suggested that the duration of  $\mu\text{g}$  may have been insufficient since the flame structures were still slowly evolving at the end of the drop test.

#### 2. Aircraft Tests

Flame behavior was considerably different in aircraft tests. All flames exhibited much greater motion resulting from the higher gravity levels, as discussed more fully in Sec. IV.D. The following trends, illustrated for  $\text{CF}_3\text{Br}$ -free, lean  $\text{H}_2$ -air mixtures, were qualitatively the same for all mixtures tested.

At sufficiently low dilution ( $\geq 7.0\%$   $\text{H}_2$ ), splitting cellular flames were observed. These flames were similar to those seen in drop-tower tests but exhibited much greater bulk motion, presumably due to buoyancy. At 6.0%  $\text{H}_2$  (Fig. 3a), cell splitting was more sluggish, and the cells were elongated in the direction coincident with the gravity vector; thus it is likely that buoyancy-induced motion contributes to the elongation. At 5.0%  $\text{H}_2$  (Fig. 3b), the motion of cells led to the formation of cylindrical flame elements, which we term "flame strings"; these will be discussed further in Sec. IV.F. Flame strings eventually broke into flame balls, hence, there was a continual generation of new flame balls by this mechanism and continual extinction of flame balls in the manner discussed in Sec. IV.C. The size distribution of the balls was bimodal but not as pronounced as was found in the drop-tower experiments. This is probably due to the effect of the greater motion of flame balls in the aircraft tests on their size, as will be discussed in Sec. IV.E.2. At 4.0%  $\text{H}_2$  (Fig. 3c), the strings were much shorter and their tendency to break rather than to elongate was much greater. At 3.75%  $\text{H}_2$  (Fig. 3d), strings did not form; instead flame balls generated shortly after ignition divided without substantial elongation. At 3.5%  $\text{H}_2$  (Fig. 3e) or leaner, cell splitting occurred only during the period shortly after ignition, and the small number of flame balls that formed from these cells did not divide. It is believed that the splitting that occurred initially in these very dilute mixtures is due to the excess enthalpy provided by the spark, which caused the flames to behave temporarily like those in less dilute mixtures exhibiting sustained cell splitting. Below about 3.35%  $\text{H}_2$ , incipient flame kernels extinguished a few seconds after ignition, even with the highest energy sparks available. These sparks are sufficient to raise a ball of gas with a radius of greater than 1 cm to typical combustion temperatures. Since the flame ball radii are smaller than 1 cm, it seems that these sparks give flame balls ample opportunity to form.

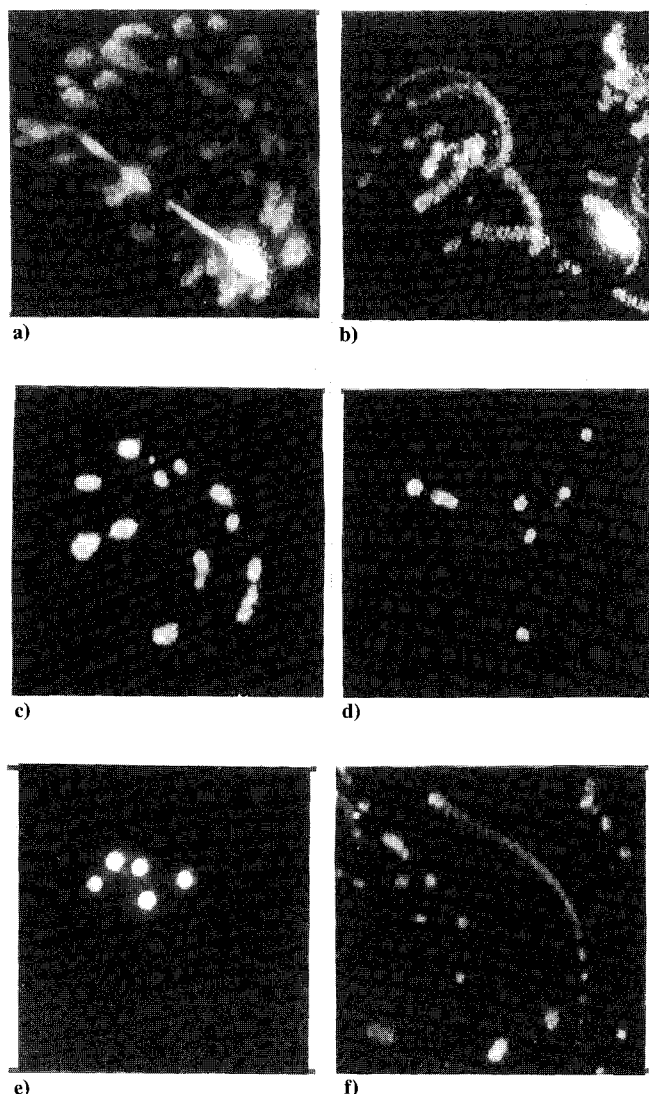


Fig. 3 Video images of flames in  $\text{CF}_3\text{Br}$ -free mixtures at  $\mu\text{g}$ . Field of view is  $15 \times 15$  cm. Spark electrodes are oriented vertically in these photographs, and the spark gap is near the center. The bright diagonal line in Fig. 3a results from the glow from thermocouple wires: a) 6.0%  $\text{H}_2$  in air; b) 5.0%  $\text{H}_2$  in air; c) 4.0%  $\text{H}_2$  in air; d) 3.75%  $\text{H}_2$  in air; e) 3.5%  $\text{H}_2$  in air; and f)  $\text{H}_2\text{-O}_2\text{-CO}_2$ ,  $\phi = 0.25$ , 7.0%  $\text{H}_2$ .

The aforementioned results were qualitatively the same over the range  $0.3 > Le > 0.06$ , with  $\text{H}_2$  and  $\text{CH}_4$  fuels, with or without added  $\text{CF}_3\text{Br}$ , and at  $2.0 > P_0 > 0.5$  atm, indicating that variations in Lewis number over this range, chemical mechanisms, and radiation spectra do not qualitatively influence these phenomena.

## B. Effects of Composition

### 1. Flammability Limits

The measured flammability limits, based on the long-duration aircraft tests, are given in Table 1. The lean  $\text{H}_2$ -air limit of  $3.35 \pm 0.05\%$   $\text{H}_2$  is close to the prediction (3.5%) of a model of flame balls<sup>16</sup> employing detailed chemical, transport, and radiative processes. For comparison, most investigations report the limit for upward flame propagation in tubes at 1 g is between 3.9 and 4.2%  $\text{H}_2$ .<sup>26</sup> Hence, for low- $Le$  mixtures, considerably more dilute mixtures are combustible at  $\mu\text{g}$ . When  $Le \approx 1$ , where flame balls do not form, the difference between the 1-g and  $\mu\text{g}$  limits is smaller, e.g., 5.1%  $\text{CH}_4$  in air at  $\mu\text{g}$ <sup>15</sup> vs 5.35% at 1-g.<sup>5,26</sup> To our knowledge, literature values are not available for the 1-g upward limits of the other mixture families tested in this work.

The time-varying nature of  $g$  in the aircraft tests did not allow a determination of whether the widest flammability limits occur at  $g = 0$  or some intermediate value  $0 < g < g_0$ . In some nonpremixed flames, it has been inferred<sup>27</sup> based on 1-g and  $\mu\text{g}$  experiments that the widest range of flammable compositions occurs at  $0 < g < g_0$  because of the ways in which buoyancy influences the transport zone thickness and the radiative losses (which in turn depends on the transport zone thickness). However, a theory of the combined effects of flow and radiative loss on flame balls<sup>7</sup> does not predict this type of behavior; instead it predicts that flow and radiation act as independent and additive loss mechanisms.

### 2. Stability Regimes

As in previous work,<sup>8</sup> stable flame balls were observed only near extinction limits. Table 1 indicates the range of mixtures exhibiting stable flame balls in the aircraft tests at times during the tests when  $g < 0.005g_0$ . Further discussion of flame ball stability is deferred to Sec. IV.C.

### 3. Measured Temperatures

Our thermocouple measurements revealed two unusual phenomena. First, it was found that, near the flammability limit, the observed temperature rise ( $T_* - T_0$ ) could greatly exceed the homogeneous adiabatic value ( $T_{\text{ad}} - T_0$ ). With  $T_*$  defined as the highest measured temperature for a given mixture and using the computed value of  $T_{\text{ad}}$  for the mixture, the largest values of  $(T_* - T_0)/(T_{\text{ad}} - T_0)$  found were about 4 for the lean  $\text{H}_2\text{-O}_2\text{-SF}_6$  mixtures. Second,  $T_*$  was found to decrease slightly with increasing fuel concentration, whereas of course  $T_{\text{ad}}$  increases with fuel concentration. For example, in  $\text{H}_2$ -air mixtures the maximum recorded temperature was found to decrease from about 1040 to 980 K as the fuel concentration was increased from 4.0 to 6.0%. This latter observation should be regarded as tentative, however, because the finite  $g$  effects and splitting processes cause the flame balls to move unpredictably. Consequently, the balls may not directly contact the thermocouple junctions, and therefore measurements may not accurately reflect the peak temperatures in these flames.

Theory provides a means of interpreting these unusual observations. It is predicted that the adiabatic flame-front temperature of a flame ball  $T_b$  is given by<sup>1-3</sup>

$$T_b = T_0 + (T_{\text{ad}} - T_0)/Le \quad (2)$$

which is larger than  $T_{\text{ad}}$  when  $Le < 1$ , as in all of the mixtures tested in this study. Moreover, Eq. (2) predicts that  $T_b$  increases with decreasing  $Le$ , which is consistent with our observation that the most pronounced superadiabatic behavior was found in the mixtures with the lowest  $Le$ , namely the lean  $\text{H}_2\text{-O}_2\text{-SF}_6$  mixtures. Of course, the nonadiabatic flame temperature  $T_*$  is less than  $T_b$ , but both theory and computation<sup>16</sup> show that near the limits the difference between  $T_b$  and  $T_*$  is small for the stable branch of solutions (i.e., the large flame balls). More importantly, on this branch  $T_*$  is predicted<sup>16</sup> to decrease slightly with increasing fuel concentration, which is consistent with the experimental observations.

It may be noted that the limit compositions shown in Table 1 for the  $\text{H}_2\text{-O}_2$ -diluent mixtures correspond to values of  $T_{\text{ad}}$  far below the  $\text{H}_2\text{-O}_2$  explosion limit temperature at 1 atm of about 850 K.<sup>5</sup> This indicates that these mixtures cannot exhibit planar flames. Most likely they are flammable only because flame balls have flame temperatures higher than  $T_{\text{ad}}$  when  $Le < 1$ . Consequently, flame balls are more robust than planar flames in mixtures with  $Le < 1$ .

### 4. Effect of Equivalence Ratio

As was discussed in Sec. II.C, a set of near-limit  $\text{H}_2\text{-O}_2\text{-N}_2$  mixtures ( $\phi_c \approx 0.32$ ) with  $0.099 < \phi < 0.4$ , each having 4.0%  $\text{H}_2$  and thus virtually the same  $T_{\text{ad}}$  (631 K) and  $Le$ , was studied

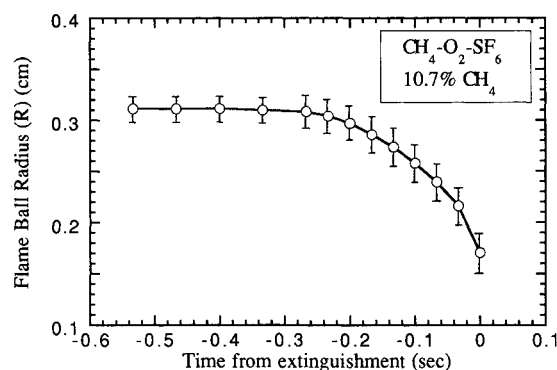


Fig. 4 Example of the dynamics of extinguishing flame balls. Mean (data points) and standard deviation (error bars) of flame ball radii vs time from extinguishment for 14 flame balls are shown. Mixture:  $\text{CH}_4\text{-O}_2\text{-SF}_6$ ,  $\phi = 1.00$ , 10.7%  $\text{CH}_4$ .

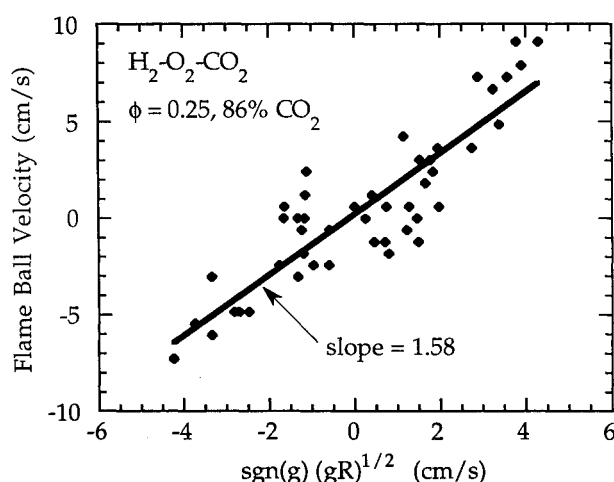


Fig. 5 Effect of instantaneous gravity level on flame ball drift velocity in aircraft tests for  $g$  and  $V$  components aligned with spark electrodes. Only one flame ball was present in this test (solid line: linear least-squares fit to data). Mixture:  $\text{H}_2\text{-O}_2\text{-CO}_2$ ,  $\phi = 0.25$ , 4.7%  $\text{H}_2$ .

in aircraft tests to assess the effects of  $\phi$  on flame balls. (Note that 4.0%  $\text{H}_2$  with  $\phi = 0.099$  corresponds to 4.0%  $\text{H}_2$  in air.) As  $\phi$  was increased from 0.099 to 0.33 by replacing  $\text{O}_2$  with  $\text{N}_2$ , the maximum observed  $R$  grew from about 0.5 to 1.0 cm, the measured luminosity decreased by nearly an order of magnitude, and the maximum observed temperature decreased from 1030 to 860 K. At  $\phi = 0.40$ , the mixture could not be ignited at all, even with the largest spark energies available.

These observations are consistent with theory,<sup>19</sup> which predicts that, for  $Le_{fu} < Le_{ox}$  and fixed  $T_{ad}$ ,  $T_*$  decreases (thus the luminosity decreases) and  $R$  increases with increasing  $\phi$ . (Of course, the caveat about temperature measurements mentioned in the preceding section should be noted.) According to Eq. (2), for  $\phi \ll \phi_c$ , where  $Le = Le_{fu} \approx 0.29$ ,  $T_b \approx 1441$  K for the family of mixtures employed here, which is well above the typical explosion limit temperature. On the other hand, for  $\phi \gg \phi_c$ , where  $Le = Le_{ox} \approx 0.91$ ,  $T_b \approx 664$  K, which is well below the explosion limit temperature. Hence, only for  $\phi \leq \phi_c$  would flammability be expected. Thus, experiments are consistent with the prediction<sup>19</sup> that a change in flame structure from fuel-deficient to oxygen-deficient burning occurs at  $\phi \approx \phi_c$ , which in turn results in a significant change in the characteristics of flame balls.

#### 5. Diffusive-Thermal vs Preferential Diffusion Models of Cellular Flames

As discussed in Sec. II.D, a set of rich ( $\phi = 2$ )  $\text{H}_2\text{-O}_2\text{-SF}_6$  mixtures was studied to test competing theories of cellular

flame formation. Pronounced cellular structures away from the limits and flame balls near the limits were observed, similar to those observed in all other low- $Le$  mixtures tested. This supports diffusive-thermal but not preferential diffusion models. Our observations of cells and flame balls in stoichiometric  $\text{CH}_4\text{-O}_2\text{-SF}_6$  mixtures also support the diffusive-thermal but not the preferential diffusion model since there is no "deficient reactant" in this case. Furthermore, studies<sup>10</sup> of lean ( $\phi = 0.5$ )  $\text{H}_2\text{-O}_2\text{-He}$  mixtures ( $Le_{fu} \approx 0.97$ ) revealed no cellular structures, which is also consistent with the diffusive-thermal but not the preferential diffusion model. We believe preferential diffusion hypotheses are limited since instability damping by thermal diffusion<sup>12,20</sup> is not considered therein.

#### C. Stability and Extinguishment Characteristics of Flame Balls

In the aircraft tests, the larger flame balls appeared to be stable, extinguishing only when the gravity levels were sufficiently high or when they drifted into the chamber walls, whereas the smaller balls would generally shrink very slowly for several seconds, then shrink more rapidly, and extinguish. An example of the dynamics of extinguishment of the small balls is shown in Fig. 4. The characteristic time for the final collapse of flame balls was about 0.3 s for the case shown in Fig. 4, about 0.2 s in near-limit  $\text{H}_2\text{-O}_2\text{-CO}_2$  mixtures, and about 0.15 s in near-limit  $\text{H}_2\text{-air}$  mixtures.

The observation that small flame balls shrink slowly at first and then extinguish rapidly is consistent with theoretical predictions of unsteady flame ball dynamics.<sup>14</sup> Physically this behavior arises because when  $Le < 1$  and the flame ball is supported by chemical reaction, it evolves on a slow time scale of order  $\beta^2 R^2 / \alpha$  where in this case  $\beta = E / RT_b \gg 1$ . In contrast, once the reaction ceases, which should occur abruptly when a fractional temperature drop of order  $1/\beta$  occurs,<sup>13,14</sup> the flame ball evolves on the faster purely diffusive time scale  $R^2 / \alpha$ . The existence of two disparate time scales could explain why small flame balls seemed stable in drop-tower tests; there was insufficient  $\mu g$  duration to witness the slow evolution followed by rapid extinguishment.

In the  $\text{H}_2\text{-air}$  case, near the limit  $R \approx 0.4$  cm and at  $T = T_*$ ,  $\alpha \approx 2$   $\text{cm}^2/\text{s}$ , hence  $R^2 / \alpha \approx 0.08$  s, which is comparable to the experimentally observed time for collapse. The longer time for extinguishment in the  $\text{CO}_2$ - and  $\text{SF}_6$ -diluted mixtures is consistent with their relative values of  $R$  and  $\alpha$  as compared with  $\text{H}_2\text{-air}$  mixtures. Hence, the observed characteristics of the final extinguishment process are consistent with the notion that chemical reaction is no longer supporting the ball and pure thermal decay prevails.

The flame ball stability results shown in Table 1 are conditioned on the restriction that  $g < 0.005g_0$ . It was necessary to condition the results in this way because the motion of the flame balls was found to influence their stability. Specifically, in mixtures near the limit for stable balls, ball splitting was most frequent when the drift velocity of the flame balls was low, i.e., when  $g$  was low. This observation is consistent with the theoretical prediction<sup>7</sup> that hydrodynamic strain acts much like heat loss in that greater strain (due to greater drift velocity) inhibits ball splitting.

#### D. Motion of Flame Balls

The drift velocities of flame balls observed in aircraft tests correlated well with  $g$  according to  $Fr \equiv V / \sqrt{gR} = \text{const}$ . An example of this correlation is shown in Fig. 5. The least-squares fit line nearly passes through the origin as expected. The value of  $Fr$  for all tests was  $1.5 \pm 0.2$ , which is consistent with the value of 1.7 found for the rising cap-shaped flames at  $1-g$ .<sup>4,5</sup>

The relation  $V / \sqrt{gR} = \text{const}$  is consistent with bubble theory,<sup>28,29</sup> which predicts  $V / \sqrt{gR} (\Delta\rho / \rho_0) = \text{const}$ , where  $\Delta\rho$  indicates the density difference between reactants and products. Whereas for a bubble characterized by  $\Delta\rho / \rho_0 \approx 1$  and a sharp interface between high- and low-density regions a value of

$Fr \approx 2/3$  would be expected,<sup>28</sup> the temperature outside the flame ball varies with radius as  $r^{-3}$

$$T(r) = T_0 + (T_* - T_0)(R/r) \quad (3)$$

Consequently, the regions of high temperature and low density extend well outside  $r = R$ , and thus the expected value of  $Fr$  would be larger than  $2/3$ . (One can define an "equivalent buoyant radius" of the flame ball  $R_{eq}$  so that  $V/\sqrt{gR_{eq}} = 2/3$ ; since  $Fr \approx 1.5$ ,  $R_{eq}/R = [1.5/(2/3)]^2 \approx 5.1$ .)

## E. Size of Flame Balls

### 1. Effect of Composition

As shown in Figs. 6a and 6b, it was found that flame ball or cell radii  $R$  were not strongly dependent on composition and the range between the largest and smallest  $R$  was narrowest in mixtures near the limit. In these figures, for conditions where the large flame balls were not stable, the larger values of  $R$  shown correspond to those just before the beginning of the splitting process. Since the smaller balls are unstable, the smaller values of  $R$  shown indicate the value before the rapid decrease in  $R$  toward extinction (i.e., as shown in Fig. 4). As will be discussed in the following section,  $g$  affected flame ball drift velocity and thereby  $R$ . Hence, only the values of  $R$  measured at times when  $g < 0.005g_0$  are reported in Figs. 6a and 6b.

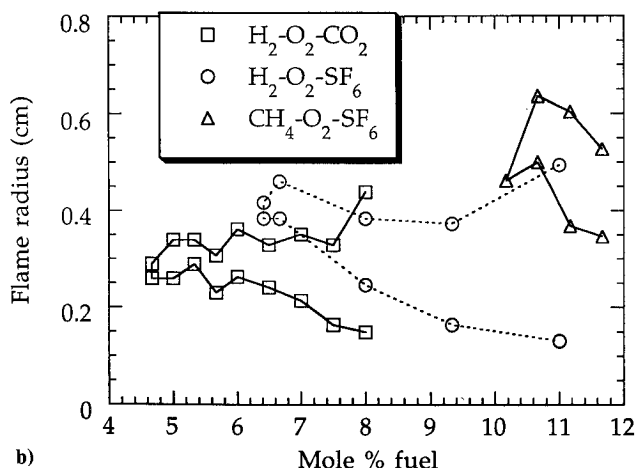
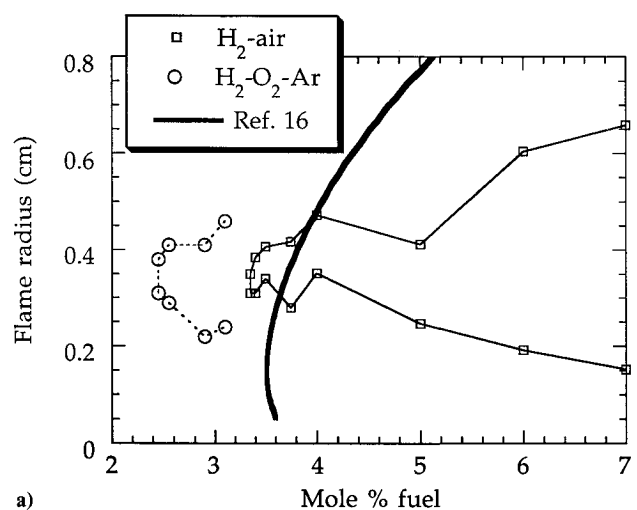


Fig. 6 Effect of dilution on cell or flame ball size and stability in  $CF_3Br$ -free mixtures. For each mixture, two sizes are shown, indicating the largest and smallest radii observed (see text). a)  $H_2$ -air mixtures and  $\phi = 0.25$   $H_2$ - $O_2$ -Ar mixtures (heavy solid curve: computational predictions<sup>16</sup> for  $H_2$ -air mixtures) and b)  $\phi = 0.25$   $H_2$ - $O_2$ - $CO_2$ ,  $H_2$ - $O_2$ - $SF_6$ , and  $CH_4$ - $O_2$ - $SF_6$  mixtures

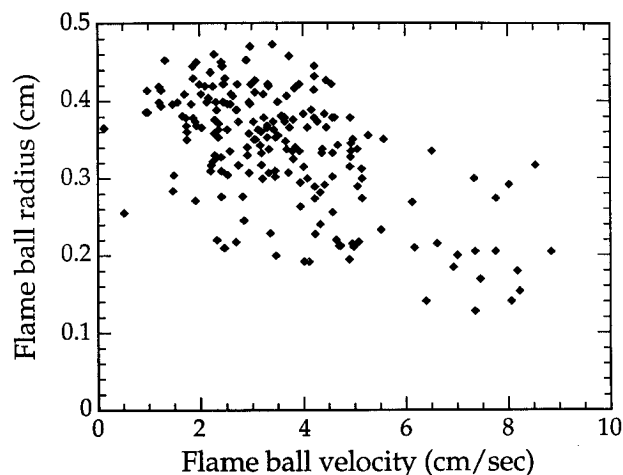


Fig. 7 Effect of flame ball drift velocity (vector sum of both observable velocity components) on flame ball size. Data from three balls are shown. Mixture:  $H_2$ - $O_2$ - $SF_6$ ,  $\phi = 0.25$ , 7.0%  $H_2$ .

Although the narrowing of the difference between the largest and smallest  $R$  as the limit is approached is qualitatively consistent with theoretical predictions,<sup>13,14</sup> it is not practical to make quantitative comparisons with theory. This is because some of the theoretical assumptions are not satisfied by the experiments. These assumptions include single-step Arrhenius kinetics with large  $\beta$ , constant thermodynamic and transport properties, and no radiation in the region immediately surrounding the flame ball.

For  $H_2$ -air flame balls, the only case where detailed numerical results are available,<sup>16</sup> the computed value of  $R$  at the flammability limit is smaller than the experimental observation, and the computed variation in flame ball size with composition is much too large (see Fig. 6a). The latter problem was also encountered when rough comparisons of theory<sup>13,14</sup> to experimental observations were made for the other mixtures.

One possible cause of the discrepancy between computation and experiment is the difference in the definition of  $R$ . In the computation the radius was defined as the location of peak OH concentration. Since this information was not available in our experiments, a comparison was made between the measured intensity profile of the  $\approx 823$ -nm radiation and that predicted based on the computation. To predict this intensity requires the temperature and  $H_2O$  concentration profiles from the computation, the emissive power as a function of temperature at 823 nm based on the Planck function, and a simple ray-tracing algorithm. A sample comparison of modeled and observed intensity profiles is shown in Fig. 2. The general shape is similar, but still the characteristic radii are very different. Similar inequities were found for other  $H_2$ -air mixtures. The discrepancies between model and experiment might occur because the reaction rate parameters of  $H_2$ - $O_2$  systems are not well known at these low flame temperatures; other investigators<sup>30</sup> have encountered similar difficulties.

### 2. Effect of Drift Velocity

The  $R$  tended to decrease with increasing  $V$ . An example of this effect is shown in Fig. 7. This trend is consistent with theoretical predictions of the effect of hydrodynamic shear or strain on flame balls.<sup>7</sup> Although the data show considerable scatter, the trend was consistent for all mixtures tested. Uncertainties in the position and velocity component in the third dimension, discussed in Sec. III, probably contribute to this scatter.

## F. Flame Strings

As was discussed in Sec. IV.A.2, structures termed "flame strings" (Figs. 3b and 3f) were observed in aircraft tests at



dilutions intermediate between those producing propagating, splitting cellular fronts and those producing isolated flame balls. Strings formed initially when flame balls were drawn through fresh mixture, forming a short cylinder that subsequently elongated. Often the end result was a cylinder with a length more than 20 times its diameter. Once formed, flame strings did not exhibit significant radial evolution; instead, they inevitably developed axial corrugations that led to their breakup and the formation of nearly equally spaced flame balls. Breakup could occur either almost simultaneously along the entire length of the string, as happened for the strings shown in Fig. 3b about 0.5 s after the image shown was taken, or quasisteadily as the string elongated at one end as it shed flame balls at the other end (Fig. 3f). Either way, the ratio of flame ball spacing to diameter just after breakup was  $3 \pm 1$ . The resulting flame balls could exhibit any behavior characteristic of the parent flame ball that formed the string, including forming another string.

Buoyant convection was probably partly responsible for the existence of flame strings because both the formation and especially the breakup of flame strings correlated with rapid changes in  $g$ . This is also consistent with the fact that strings were not observed in drop-tower tests, which had much lower  $g$  levels. Generally strings broke when  $g$  decreased suddenly, which is consistent with theory,<sup>31</sup> which predicts that convective transport enhances the stability of flame strings to the corrugations that cause their breakup.

The existence of flame strings is curious because the solution in cylindrical geometry corresponding to Eq. (3) is of the form  $T(r) = a + b \ln(r)$ , where  $a$  and  $b$  are constants. Consequently, no steady, convection-free cylindrical flames are possible because the boundary conditions cannot be satisfied without singularities as  $r \rightarrow \infty$ . Thus, the flame string should be in a continual state of radial evolution. Since the singularity that rules out the steady solution is weak (logarithmic), it is possible that the time scale of radial evolution is slow compared with the time scales for both 1) the buoyancy-induced motion of flame balls which draws out their reactive surfaces and forms strings and 2) the corrugations that break the strings. Unfortunately, it is difficult to test this hypothesis because the mathematical problems associated with the singularity make it hard to identify a time scale for this radial evolution that could be compared with the two other relevant time scales.

## V. Concluding Remarks

### A. Summary of Results

Microgravity experiments with low- $Le$  mixtures in drop towers and aircraft suggest the existence of stable, stationary flame balls. These structures do not exhibit self-propagation, as indicated by their absence of movement in drop-tower tests and  $g$ -level-dependent drift velocity in aircraft tests. Convective motion of flame balls is neither necessary nor desirable for their existence and survival. Moreover, convection appears to weaken them, as evidenced by their smaller size and increased extinguishment tendency at higher drift velocity and the significantly wider flammability limits at  $\mu g$  than at  $1 g$ .

Mixture composition has a substantial effect on the behavior of flame balls. For mixtures sufficiently far from flammability limits, flame balls consistently split into more flame balls. For more dilute mixtures closer to the flammability limits, stable "large" flame balls are observed, whereas "small" flame balls shrink and eventually extinguish, probably aided by convective motions. For still more dilute mixtures all flames extinguish, regardless of convection. Additionally, a change in flame ball behavior, probably corresponding to a transition from locally lean to locally rich burning, is observed near  $\phi = \phi_c \equiv Le_{fu}/Le_{ox}$  rather than at  $\phi = 1$  (as in planar flames).

Qualitative comparison of experimental results with theoretical predictions suggests that most of these phenomena can be described by the interactions of Lewis number effects and

radiant heat loss with the spherical geometry of flame balls. Based on comparisons of flames in mixtures having various chemical properties, chemical reaction mechanisms do not seem to govern the qualitative features of these phenomena.

For mixture compositions intermediate between those producing propagating cellular fronts and those producing stable flame balls, a new structure, termed flame strings, was observed. This structure probably results from buoyancy-induced motions of flame balls. Flame strings are unstable to axial corrugations but are relatively long lived. Their existence might be interpreted considering their relative time scales for formation vs radial evolution.

### B. Open Issues

There are several unresolved matters concerning the existence and stability of stationary spherical and cylindrical flames at  $\mu g$ . A detailed numerical model thought to contain all of the ingredients necessary to predict flame ball behavior was in good qualitative but poor quantitative agreement with the experiments. The most significant limitation of the experiments is the relatively poor quality of  $\mu g$  in the aircraft tests. This may compromise the validity of quantitative comparisons of observed flame ball properties with computations. Also, because of the poor quality of  $\mu g$  in the aircraft tests and the short duration of drop-tower tests, it is not certain which factor(s), convection and/or long  $\mu g$  durations, is/are necessary to observe flame strings. Consequently, long-duration low-gravity tests, for example on orbiting spacecraft, are desirable.

### C. Practical Perspective

Besides providing an assessment of the influences of buoyancy on flames at  $1 g$ , our experiments may be relevant to the assessment of fire safety in manned spacecraft, where a variety of fault scenarios could lead to gaseous fuels, e.g., from propellant tanks or fuel cells, coming into contact with oxidizing atmospheres in inhabited spaces. Our experiments may also be relevant to the combustion of lean  $H_2$ -air mixtures in strongly turbulent flows because, as discussed in Sec. IV.B.3, in mixtures with low  $Le$ , flame balls are more robust structures than planar flames. Thus, sufficiently strong turbulence may extinguish plane flames,<sup>32</sup> whereas flame balls could persist under the same conditions. Consequently, structures reminiscent of flame balls or flame strings could be the prevalent ones in near-limit turbulent combustion of lean  $H_2$ -air mixtures.

## Acknowledgments

This work was supported by the NASA Lewis Research Center under Grants NAG3-965, NAG3-1242, and NAG3-1523. We thank Ruey-Hung Chen and Eric Roegner at Princeton University, Robert Williams and Linda White at NASA Johnson Space Center, and Robert Shurney and Jeffrey Mullins at NASA Marshall Space Flight Center for their assistance with the KC-135A flight experiments.

## References

- <sup>1</sup>Zeldovich, Y. B., *Theory of Combustion and Detonation of Gases*, Academy of Sciences (USSR), Moscow, 1944.
- <sup>2</sup>Buckmaster, J. D., and Weeratunga, S., "The Stability and Structure of Flame Bubbles," *Combustion Science and Technology*, Vol. 35, Nos. 3 and 4, 1984, pp. 287-296.
- <sup>3</sup>Deshaies, B., and Joulin, G., "On the Initiation of a Spherical Flame Kernel," *Combustion Science and Technology*, Vol. 37, Nos. 3 and 4, 1984, pp. 99-116.
- <sup>4</sup>Bohm, G., and Clusius, K., *Zeitschrift für Naturforschung*, Vol. 3A, 1948, pp. 386-393.
- <sup>5</sup>Lewis, B., and von Elbe, G., *Combustion, Flames, and Explosions of Gases*, 3rd ed., Academic Press, Orlando, FL, 1987, Chap. 5.
- <sup>6</sup>Weeratunga, S., Buckmaster, J. D., and Johnson, R. E., "A Flame-Bubble Analogue and its Stability," *Combustion and Flame*, Vol. 79, No. 1, 1990, pp. 100-109.
- <sup>7</sup>Buckmaster, J. D., and Joulin, G., "Flame Balls Stabilized by



Suspension in Fluid with a Steady Linear Ambient Velocity Gradient," *Journal of Fluid Mechanics*, Vol. 227, 1991, pp. 407-427.

<sup>8</sup>Ronney, P. D., "Near-Limit Flame Structures at Low Lewis Number," *Combustion and Flame*, Vol. 82, No. 1, 1990, pp. 1-14.

<sup>9</sup>Mitani, T., and Williams, F., "Studies of Cellular Flames in Hydrogen-Oxygen-Nitrogen Mixtures," *Combustion and Flame*, Vol. 39, No. 2, 1980, 169-190.

<sup>10</sup>Ronney, P. D., "On the Mechanisms of Flame Propagation Limits and Extinction Processes at Microgravity," *22nd Symposium (International) on Combustion*, Combustion Inst., Pittsburgh, PA, 1988, pp. 1615-1623.

<sup>11</sup>Abbud-Madrid, A., and Ronney, P. D., "Effects of Radiative and Diffusive Transport Processes on Premixed Flames Near Flammability Limits," *23rd Symposium (International) on Combustion*, Combustion Inst., Pittsburgh, PA, 1990, pp. 423-431.

<sup>12</sup>Williams, F. A., *Combustion Theory*, 2nd ed., Benjamin-Cummings, Menlo Park, CA, 1985, Chaps. 5 and 9.

<sup>13</sup>Buckmaster, J. D., Joulin, G., and Ronney, P. D., "Effects of Heat Loss on the Structure and Stability of Flame Balls," *Combustion and Flame*, Vol. 79, Nos. 3 and 4, 1990, pp. 381-392.

<sup>14</sup>Buckmaster, J. D., Joulin, G., and Ronney, P. D., "Structure and Stability of Non-adiabatic Flame Balls: II. Effects of Far-Field Losses," *Combustion and Flame*, Vol. 84, Nos. 3 and 4, 1991, pp. 411-422.

<sup>15</sup>Lee, C., and Buckmaster, J. D., "The Structure and Stability of Flame Balls: A Near-Equidiffusional Flame Analysis," *SIAM Journal on Applied Mathematics*, Vol. 51, No. 5, 1991, pp. 1315-1326.

<sup>16</sup>Buckmaster, J. D., and Smooke, M., "Analytical and Numerical Modelling of Flame-Balls in Hydrogen-Air Mixtures," *Combustion and Flame*, Vol. 94, No. 1, 1993, pp. 113-124.

<sup>17</sup>Fenimore, C., and Jones, G., "Decomposition of Sulphur Hexafluoride in Flames by Reaction with Hydrogen Atoms," *Combustion and Flame*, Vol. 8, No. 2, 1964, pp. 231-234.

<sup>18</sup>Wray, K. L., and Feldman, E. V., "The Pyrolysis and Subsequent Oxidation of SF<sub>6</sub>," *14th Symposium (International) on Combustion*, Combustion Inst., Pittsburgh, PA, 1972, pp. 229-238.

<sup>19</sup>Joulin, G., "Preferential Diffusion and the Initiation of Lean Flames of Light Fuels," *SIAM Journal on Applied Mathematics*, Vol. 47, No. 5, 1987, pp. 998-1016.

<sup>20</sup>Sivashinsky, G. I., "Diffusional-Thermal Theory of Cellular Flames," *Combustion Science and Technology*, Vol. 15, Nos. 3 and

4, 1977, pp. 137-145.

<sup>21</sup>Hertzberg, M., "Selective Diffusional Demixing: Occurrence and Size of Cellular Flames," *Progress in Energy and Combustion Science*, Vol. 15, No. 3, 1989, pp. 203-239.

<sup>22</sup>Patnaik, G., Kailasanath, K., Laskey, K., and Oran, E., "Detailed Numerical Simulations of Cellular Flames," *22nd Symposium (International) on Combustion*, Combustion Inst., Pittsburgh, PA, 1988, pp. 1517-1526.

<sup>23</sup>Microgravity Combustion Group, "Microgravity Combustion Science: Progress, Plans, and Opportunities," NASA TM-105410, April 1992.

<sup>24</sup>Weiland, K. J., "Intensified Array Camera Imaging of Solid Surface Combustion Aboard the NASA Learjet," AIAA Paper 92-0240, also *AIAA Journal*, Vol. 31, No. 4, 1993, pp. 786-788.

<sup>25</sup>Herzberg, G., *Infrared and Raman Spectra*, van Nostrand Reinhold, New York, 1950, p. 281.

<sup>26</sup>Coward, H., and Jones, C., "Flammability Limits of Gases and Vapors," *U. S. Bureau of Mines Bulletin 503*, 1952.

<sup>27</sup>Olson, S. L., Ferkul, P. V., and Tien, J. S., "Near-Limit Flame Spread Over a Thin Solid Fuel in Microgravity," *22nd Symposium (International) on Combustion*, Combustion Inst., Pittsburgh, 1988, pp. 1213-1222.

<sup>28</sup>Batchelor, G. K., *An Introduction to Fluid Dynamics*, Cambridge Univ. Press, Cambridge, England, UK, 1967, p. 476.

<sup>29</sup>Davies, R. M., and Taylor, G. I., "The Mechanics of Large Bubbles Rising Through Extended Liquids and Through Liquids in Tubes," *Proceedings of the Royal Society (London), Mathematical and Physical Sciences*, Series A, Vol. 200, 1950, pp. 375-390.

<sup>30</sup>Egolfopoulos, F. N., and Law, C. K., "An Experimental and Computational Study of the Burning Rates of Ultra-Lean to Moderately-Rich H<sub>2</sub>/O<sub>2</sub>/N<sub>2</sub> Laminar Flames with Pressure Variations," *23rd Symposium (International) on Combustion*, Combustion Inst., Pittsburgh, PA, 1990, pp. 333-340.

<sup>31</sup>Buckmaster, J. D., "A Flame-String Model and Its Stability," *Combustion Science and Technology*, Vol. 84, Nos. 3 and 4, 1992, pp. 163-176.

<sup>32</sup>Abdel-Gayed, R. G., and Bradley, D., "Criteria for Turbulent Propagation Limits of Premixed Flames," *Combustion and Flame*, Vol. 62, No. 1, 1985, pp. 61-68.

<sup>33</sup>Hirschfelder, J. O., Curtiss, C. F., and Bird, R. B., *Molecular Theory of Gases and Liquids*, Wiley, New York, 1954, Sec. 8.4.